Published in final edited form as:
Biochem Biophys Res Commun. 2013 September 6; 438(4): 600–606. doi:10.1016/j.bbrc.2013.08.009.

Induction of human breast cell carcinogenesis by triclocarban and intervention by curcumin

Shilpa Sood, **Shambhunath Choudhary**, and **Hwa-Chain Robert Wang***
Anticancer Molecular Oncology Laboratory, Department of Biomedical and Diagnostic Sciences, College of Veterinary Medicine, University of Tennessee, Knoxville, TN, USA

Abstract

More than 85% of breast cancers are sporadic and attributable to long-term exposure to environmental carcinogens and co-carcinogens. To identify co-carcinogens with abilities to induce cellular pre-malignancy, we studied the activity of triclocarban (TCC), an antimicrobial agent commonly used in household and personal care products. Here, we demonstrated, for the first time, that chronic exposure to TCC at physiologically-achievable nanomolar concentrations resulted in progressive carcinogenesis of human breast cells from non-cancerous to pre-malignant. Pre-malignant carcinogenesis was measured by increasingly-acquired cancer-associated properties of reduced dependence on growth factors, anchorage- independent growth and increased cell proliferation, without acquisition of cellular tumorigenicity. Long-term TCC exposure also induced constitutive activation of the Erk–Nox pathway and increases of reactive oxygen species (ROS) in cells. A single TCC exposure induced transient induction of the Erk–Nox pathway, ROS elevation, increased cell proliferation, and DNA damage in not only non-cancerous breast cells but also breast cancer cells. Using these constitutively- and transiently-induced changes as endpoints, we revealed that non-cytotoxic curcumin was effective in intervention of TCC-induced cellular pre-malignancy. Our results lead us to suggest that the co-carcinogenic potential of TCC should be seriously considered in epidemiological studies to reveal the significance of TCC in the development of sporadic breast cancer. Using TCC-induced transient and constitutive endpoints as targets will likely help identify non-cytotoxic preventive agents, such as curcumin, effective in suppressing TCC-induced cellular pre-malignancy.

Keywords

Breast cell carcinogenesis; Curcumin; Prevention; TCC

1. Introduction

Breast cancer is the most common cancer and the second leading cause of cancer deaths among women in northern America and Europe [1]. More than 85% of breast cancers are sporadic and attributable to long-term exposure to small quantities of environmental carcinogenic agents that progressively induce non-cancerous cells to pre-malignancy to malignancy in a multi-step and multi-path disease process [2–5]. Over 200 chemical mammary carcinogens have been identified by measuring their ability to intensively induce malignant cells or tissues [6]. While carcinogens are capable of inducing cellular malignancy, co-carcinogens are capable of inducing cell pre-malignancy or enhancing

*Corresponding author. Address: Department of Biomedical and Diagnostic Sciences, College of Veterinary Medicine, University of Tennessee, 2407 River Drive, Knoxville, TN 37996, USA. Fax: +1 865 974 5616. hcrwang@utk.edu (H.-C. R. Wang).

cellular malignancy. Investigations into co-carcinogens, at low-doses (pico-to nano-molar), capable of chronically inducing cellular pre-malignancy have been overlooked in past studies of breast cancer development and prevention.

One potential co-carcinogen triclocarban (TCC; 3,4,4′-trichlorocarbanilide) is a lipophilic, antimicrobial compound widely used in household and personal care products, such as disinfectants, soaps, deodorants, and detergents, etc. [7]. TCC exhibits endocrine-disrupting activity to induce estradiol-dependent activation of estrogen receptor (ER)-responsive gene expression but alone lacks agonistic activity [8,9]. Direct dermal exposure to TCC results in transdermal absorption and accumulation in underlying tissues, including mammary tissues [10]. More specifically, a single whole-body shower using TCC-containing soap results in blood levels as high as ~500 nM within 3 h [11,12]. In addition, TCC is resistant to both wastewater chemical and biological treatments, and agricultural use of TCC-containing biosolids renders TCC into the food chain, thus increasing human exposure to TCC [7,13–15]. Although the role of TCC in increasing breast cancer risk has been questioned, it has not yet been addressed. It is imperative to understand the role of low-dose TCC in sporadic breast cancer development and to identify effective agents for intervention.

Curcumin, the major phenolic compound in turmeric extracts, has been used in Asian countries for hundreds of years to treat various diseases, including gastrointestinal and rheumatic disorders, as well as inflammation and cancer [16]. It has been shown that curcumin inhibits growth and metastasis of breast cancer cells both *in vitro* and *in vivo* [17,18]. Curcumin inhibits stomach tumors induced by benzo[a]pyrene (B[a]P) in mice [19], genotoxicity induced by heterocyclic amines in *Salmonella typhimurium* [20], and bioactivation of B[a]P-diol in oral squamous carcinoma cells [21]. However, the activity of curcumin in prevention of sporadic breast cancer has not been fully addressed.

We have developed a cellular model to identify carcinogenic agents, at physiologically-achievable levels, capable of chronically inducing human breast epithelial cell carcinogenesis [22–24]. We revealed that cellular, biochemical, and molecular changes transiently induced by single exposure to carcinogenic agents, and changes constitutively induced by cumulative exposures play essential roles in induction of cellular carcinogenesis and maintenance of acquired cancer-associated properties, respectively [22–24]. We then used these transient and constitutive changes/endpoints as targets to identify non-cytotoxic agents, such as green tea catechins and grape seed extract, effective in intervention of cellular carcinogenesis [22–24]. In this communication, we used our model system, for the first time, to reveal the ability of TCC, at nanomolar levels, to induce breast cell pre-malignancy. We also studied the activity of curcumin, at non-cytotoxic levels, effective in intervention of TCC-induced cellular carcinogenesis.

2. Materials and methods

2.1. Cell cultures and reagents

MCF10A (American Type Culture Collection [ATCC], Rockville, MD) and derived cell lines were maintained in complete (CM) medium (1:1 mixture of DMEM and HAM's F12, supplemented with 100 ng/mL cholera enterotoxin, 10 μg/mL insulin, 0.5 μg/mL hydrocortisol, 20 ng/mL epidermal growth factor, and 5% horse serum) [22–24]. Human breast cancer MCF7 cells (ATCC) were maintained in DMEM supplemented with 10% heat-inactivated fetal bovine serum [24]. All cultures were maintained in medium supplemented with 100 U/mL penicillin and 100 μg/mL streptomycin in 5% CO_2 at 37 °C. Stock aqueous solutions of TCC (Sigma–Aldrich, St. Louis, MO), chloromethyl-dichlorodihydrofluorescein-diacetate (CM-H_2DCF-DA) (Invitrogen, Carlsbad, CA), U0126 (Cell Signaling, Beverly, MA), and curcumin (MP Biomedicals, Solon, Ohio) were prepared

in DMSO and diluted in culture medium. Stock aqueous solutions of *N*-acetyl-*L*-cysteine (NAC) (Alexis, San Diego, CA) were prepared in H_2O and diluted in culture medium for assays.

2.2. Chronic induction of cellular carcinogenesis

Twenty-four hours after each subculturing, cells were exposed to TCC for 48 h, as one cycle of exposure for 10–20 cycles to induce cellular carcinogenesis [22–24].

2.3. Reduced dependence on growth factors

5×10^3 cells were seeded in 60-mm culture dishes and maintained in low-mitogen (LM) medium containing reduced total serum and mitogenic additives to 2% of the concentration formulated in CM medium; cell colonies (≥0.5 mm diameter) were counted [22–24].

2.4. Anchorage-independent growth

3 or 5×10^3 cells were mixed with soft-agar consisting of 0.4% SeaPlaque agarose (Sigma–Aldrich) in a mixture (1:1) of CM medium with 3 d conditioned medium prepared from MCF10A cultures, plated on top of the 2% SeaPlaque agarose base layer in a 60-mm culture dish, and maintained for 20 d to develop cell clones. Cell colonies (≥0.1 mm diameter) were counted [22–24].

2.5. Cell viability assay

A Methyl Thiazolyl Tetrazolium (MTT) assay kit (ATCC) was used to measure cell survivability. 5×10^3 cells were seeded into each well of 96-well culture plates for 24 h. After indicated treatments, cells were incubated with MTT Reagent for 4 h, followed by incubation with detergent reagent for 24 h. Reduced MTT reagent in cultures was quantified with an ELISA reader (Bio-Tek, Winooski, VT) [22–24].

2.6. Cell proliferation

Cell proliferation was determined by 5-bromo-2′-deoxyuridine (BrdU) incorporation into cellular DNA using the BrdU cell proliferation ELISA kit (Roche, Indianapolis, IN). 5×10^3 cells were seeded into each well of 96-well culture plates for 24 h. After treatment, cells were labeled with BrdU for 12 h, fixed, incubated with peroxidase- conjugated BrdU-specific antibodies, and stained with peroxidase substrate. Quantification of BrdU-labeled cells was determined with an ELISA reader (Bio-Tek) [22–24].

2.7. Intracellular ROS

As performed previously [22–24], cells were incubated with 5 μM CM-H_2DCF-DA for 1 h to detect ROS level by flow cytometry; the mean fluorescence intensity of DCF was quantified using Multicycle software (Phoenix, San Diego, CA).

2.8. DNA damage

DNA damage was measured by a comet assay [22–24]. In brief, cells were mixed with 1% low-melting agarose and placed on agarose- coated slides. After electrophoresis, slides were stained with propidium iodide and examined with a Zeiss fluorescence microscope (Thornwood, NY). Fifty nuclei per slide were scored for tail moment (% of DNA in the tail × tail length) using CometScore software (Tritek Corp., Sumerduck, VA).

2.9. Immunoblotting

Equal amounts of cellular proteins were resolved by electrophoresis in SDS–polyacrylamide gels and transferred to nitrocellulose filters for immunoblotting [22–24]. Specific antibodies

were used to detect H-Ras, phosphorylated Mek (p-Mek), Mek, p-Erk1/2, Erk1/2, Nox-1, and β-Actin (Santa Cruz, Santa Cruz, CA). Antigen– antibody complexes on filters were detected by the Supersignal chemiluminescence kit (Pierce, Rockford, IL).

2.10. Statistical analysis

The Student *t* test was used to analyze statistical significance, indicated by $^{*}P < 0.05$, $^{**}P < 0.01$, $^{***}P < 0.001$; a P value of ≤0.05 was considered significant.

3. Results and discussion

3.1. TCC induction of breast cell carcinogenesis

To investigate the ability of TCC to induce breast cell carcinogenesis, we repeatedly exposed MCF10A cells to TCC at various concentrations for 10 and 20 cycles. Normal epithelial cells require growth factors to grow and survive, and cell adhesion to extracellular matrix is essential for survival in a multi-cellular environment; in contrast, cancerous cells acquire the abilities of a reduced dependence on growth factors and an independence from cell adhesion to matrix (anchorage-independent growth) to survive [25,26]. We used these two cancer-associated properties as constitutive cellular endpoints to measure the progress of cellular carcinogenesis induced by carcinogenic agents [23,24]. As shown in Fig. 1A and B, higher numbers of survived colonies, which acquired both cancer-associated properties, remained in cultures exposed to TCC at higher concentrations than in cultures exposed to lower concentrations (1000 > 500 > 200 nM), and higher numbers of colonies survived in cultures exposed to TCC for 20 cycles than in cultures exposed for 10 cycles. These results indicate that cumulative exposures of MCF10A cells to TCC resulted in progressively-increased acquisition of these two constitutive cellular endpoints in a dose- and exposure-dependent manner.

Our previous studies [23,24] revealed that the Erk–Nox pathway, as a constitutive biochemical endpoint, is involved in maintaining constitutive cellular endpoints induced by chronic exposure to carcinogenic agents, including B[a]P, 4-(methylnitrosamino)- 1-(3-pyridyl)-1-butanone (NNK), and 2-amino-1-methyl- 6-phenylimidazo[4,5-b]pyridine (PhIP). Chronic exposure to TCC also resulted in constitutive activation of the Erk–Nox pathway, indexed by increased phosphorylation of Erk1/2 and increased level of Nox-1 (Fig. 1C); the level of induced Erk–Nox pathway was in concert with the degree of constitutive cellular endpoints (Fig. 1A and B). These results are consistent with our published findings of constitutive endpoints induced by B[a]P, NNK, and/or PhIP [23,24]. The reduced dependence on growth factors and anchorage- independent growth can also be used as constitutive cellular endpoints, and the Erk–Nox pathway can be used as a constitutive biochemical endpoint to measure TCC-induced cellular carcinogenesis.

3.2. TCC-induced transient endpoints

We reported that a single exposure of MCF10A cells to B[a]P, NNK, or PhIP induces transient endpoints, including Erk–Nox pathway activation, ROS elevation, increased cell proliferation, and DNA damage, which play essential roles in initiation of carcinogenesis in each exposure, accounting for the mechanisms of these agents in induction of carcinogenesis [23,24]. Because studies showed that a single whole-body shower using TCC-containing soap frequently results in blood levels at ~200 nM [11,12], we chose to use the physiologically-achievable level of 200 nM TCC to study its activity and mechanisms in induction of cellular carcinogenesis.

As shown in Fig. 2A, phosphorylation of Erk1/2 was transiently induced, and the maximal level of phosphorylated Erk1/2 was reached in 24 h, indicating a transient activation of the

Erk pathway by TCC. Using the Mek inhibitor U0126 to block the Erk pathway, Nox-1 was reduced to a lower level than in parental cells and TCC-exposed cells (Fig. 2B-1), indicating that TCC induced Nox-1 through activation of the Erk pathway, thereby verifying the ability of TCC to induce transient activation of the Erk–Nox pathway. Using NAC to block ROS, we detected that the Erk–Nox pathway was suppressed in TCC-exposed cells (Fig. 2B-2), indicating ROS induced by TCC in activation of the Erk–Nox pathway. Additionally, blocking the Erk–Nox pathway by U0126 resulted in significant reduction of TCC-induced ROS (Fig. 2B-3), suppression of ROS by NAC or U0126 resulted in significant reduction of TCC-induced cell proliferation (Fig. 2B-4), and blockage of the Erk–Nox pathway or ROS resulted in suppression of TCC-induced DNA damage (Fig. 2B-5). These results indicate that TCC was able to induce the Erk-Nox pathway, Nox-dependent ROS elevation, and Nox-independent ROS elevation to induce increased cell proliferation and DNA damage. TCC-induced, Nox-independent ROS also played a role in activation of the Erk–Nox pathway.

To address if TCC's ability to induce these transient endpoints was limited to the ER-negative breast MCF10A cells, we detected that TCC was able to induce the Erk–Nox pathway (Fig. 2C-1), ROS elevation (Fig. 2C-2), and DNA damage (Fig. 2C-3) in human breast cancer ER-positive MCF7 cells. The results indicate that TCC-induced transient endpoints were not specific to MCF10A cells or ER status.

3.3. TCC-induced constitutive endpoints

To assess carcinogenic potency of TCC-exposed breast cells, we used the tumorigenic P-20 cell line, which resulted from cumulative exposure of MCF10A cells to PhIP for 20 cycles [24], and a highly-tumorigenic, oncogenic Ras-expressing MCF10A-Ras cell line [24] as controls. Cumulative exposures of MCF10A cells to 200 nM TCC for 10 and 20 cycles resulted in T-10 and T-20 cell lines, respectively. We detected that the constitutive endpoints of reduced dependence on growth factors (Fig. 3A-1), anchorage-independent growth (Fig. 3A-2), increased cell proliferation (Fig. 3A-3), ROS elevation (Fig. 3A-4), and Mek–Erk–Nox pathway activation (Fig. 3A-5) were increasingly induced in T-10 and T-20 cells in an exposure-dependent manner; however, none of these constitutive endpoints was induced to a comparable level to those acquired by tumorigenic P-20 and MCF10A-Ras cells. Inoculation of T-20 cells into mammary fat pads of immunocompromised nu/nu mice did not result in any xenograft tumors in 90 days in contrast to xenograft tumors derived from P-20 and MCF10A-Ras cells, indicating that the T-20 cell line was not tumorigenic (data not shown).

To detect if long-term exposure to TCC was able to induce MCF7 cells to acquire increased degrees of cancer-associated properties, we repeatedly exposed MCF7 cells to 200 nM TCC for 10 cycles, resulting in MCF7/T10 cell line. We detected that MCF7/T10 cells acquired higher degrees of the constitutive endpoints of anchorage- independent growth (Fig. 3B-1), increased cell proliferation (Fig. 3B-2), ROS elevation (Fig. 3B-3), and Erk–Nox pathway activation (Fig. 3B-4) versus parental MCF7 cells. These results indicate that cumulative exposures of MCF7 cells to TCC enhanced cancerous properties in MCF7 cells.

3.4. Curcumin intervention of TCC-induced carcinogenesis

To identify preventive agents effective in intervention of cellular pre-malignancy induced by chronic exposure to TCC, we pursued agents, at non-cytotoxic levels, capable of blocking TCC-induced transient and constitutive endpoints in MCF10A cells. As shown in Fig. 4A, treatment with curcumin at 10 and 20 μM resulted in significant reduction of cell viability, but 0.1 or 1 μM did not result in any detectable reduction of cell viability. We used curcumin at the non-cytotoxic concentration of 1 μMin the studies of the ability of curcumin to block TCC-induced transient endpoints. We detected that co-exposure to curcumin

reduced TCC-induced transient endpoints of Erk–Nox pathway activation (Fig. 4B-1), ROS elevation (Fig. 4B-2), increased cell proliferation (Fig. 4B-3), and DNA damage (Fig. 4B-4) in a single exposure. These results indicate that co-exposure to curcumin interfered in TCC-induced initiation of cellular carcinogenesis. After 10 cycles of exposure, curcumin co-exposure significantly reduced TCC-induced constitutive endpoints of reduced dependence on growth factors (Fig. 4C-1), anchorage-independent growth (Fig. 4C-2), increased cell proliferation (Fig. 4C-3), and ROS elevation (Fig. 4C-4), as well as activation of the Erk–Nox pathway (Fig. 4C-5). Accordingly, curcumin was effective in the intervention of transient and constitutive endpoints induced by TCC in single and accumulated exposures, respectively. Thus, curcumin should be considered for early intervention of TCC-induced, cellular pre-malignancy.

American lifestyles involve wide uses of cleaning agents containing TCC and consumption of TCC-contaminated agricultural products. The role of TCC in increasing breast cancer risk has not yet been fully addressed. Our model system revealed, for the first time, that cumulative exposures of human breast cells to TCC at physiologically-achievable, nanomolar concentrations induced carcinogenesis from a non-cancerous stage to pre-malignant stages in a dose- and exposure-dependent manner, suggesting the novel ability of TCC, as a co-carcinogen, to induce breast cell pre-malignancy that should be seriously considered in epidemiological studies to reveal the significance of TCC in sporadic breast cancer development. Using TCC-induced transient and constitutive endpoints as targets enabled us to identify non-cytotoxic preventive agents, such as curcumin, effective in suppressing TCC-induced cellular pre-malignancy. However, whether TCC is able to enhance malignancy with other carcinogenic agents remains to be clarified.

Acknowledgments

We are grateful to Ms. D.J. Trent for technique support in flow cytometric analysis, Ms. M. Bailey for textual editing of the manuscript, and Dr. J. Chen for his informative support in dosing TCC at the initial stage of this research. This study was supported by the University of Tennessee, Center of Excellence in Livestock Diseases and Human Health (H.CR. Wang), and an NIH grant CA129772 (HCR Wang).

References

1. Gray J, Evans N, Taylor B, et al. State of the evidence: the connection between breast cancer and the environment. Int J Occup Environ Health. 2009; 15:43–78. [PubMed: 19267126]
2. Kelloff, GJ.; Hawk, ET.; Sigman, CC. Cancer Chemoprevention: Strategies for Cancer Chemoprevention. Humana Press; Totowa, NJ: 2005. p. 517
3. DeBruin LS, Josephy PD. Perspectives on the chemical etiology of breast cancer. Environ Health Perspect. 2002; 110:119–128. [PubMed: 11834470]
4. Hecht SS. Tobacco smoke carcinogens and breast cancer. Environ Mol Mutagen. 2002; 39:119–126. [PubMed: 11921179]
5. Guengerich FP. Metabolism of chemical carcinogens. Carcinogenesis. 2000; 21:345–351. [PubMed: 10688854]
6. Rudel RA, Attfield KR, Schifano JN, et al. Chemicals causing mammary gland tumors in animals signal new directions for epidemiology, chemicals testing, and risk assessment for breast cancer prevention. Cancer. 2007; 109:2635–2666. [PubMed: 17503434]
7. Sapkota A, Heidler J, Halden RU. Detection of triclocarban and two cocontaminating chlorocarbanilides in US aquatic environments using isotope dilution liquid. Environ Res. 2007; 103:21–29. [PubMed: 16678153]
8. Ahn KC, Zhao B, Chen J, et al. In vitro biologic activities of the antimicrobials triclocarban, its analogs, and triclosan in bioassay screens: receptor-based bioassay screens. Environ Health Perspect. 2008; 116:1203–1210. [PubMed: 18795164]

9. Chen J, Ahn KC, Gee NA, et al. Triclocarban enhances testosterone action: a new type of endocrine disruptor? Endocrinology. 2008; 149:1173–1179. [PubMed: 18048496]
10. Harvey PW, Darbre P. Endocrine disrupters and human health: could oestrogenic chemicals in body care cosmetics adversely affect breast cancer incidence in women? J Appl Toxicol. 2004; 24:167–176. [PubMed: 15211609]
11. Schebb NH, Inceoglu B, Ahn KC, et al. Investigation of human exposure to triclocarban after showering and preliminary evaluation of its biological effects. Environ Sci Technol. 2011; 45:3109–3115. [PubMed: 21381656]
12. Schebb NH, Ahn KC, Dong H, et al. Whole blood is the sample matrix of choice for monitoring systemic triclocarban levels. Chemosphere. 2012; 87:825–827. [PubMed: 22273184]
13. Coogan MA, La Point TW. Snail bioaccumulation of triclocarban, triclosan, and methyltriclosan in a North Texas, USA, stream affected by wastewater treatment plant runoff. Environ Toxicol Chem. 2008; 27:1788–1793. [PubMed: 18380516]
14. Heidler J, Sapkota A, Halden RU. Partitioning, persistence, and accumulation in digested sludge of the topical antiseptic triclocarban during wastewater treatment. Environ Sci Technol. 2006; 40:3634–3639. [PubMed: 16786704]
15. Miller TR, Heidler J, Chillrud SN, et al. Fate of triclosan and evidence for reductive dechlorination of triclocarban in estuarine sediments. Environ Sci Technol. 2008; 42:4570–4576. [PubMed: 18605588]
16. Jurenka JS. Anti-inflammatory properties of curcumin, a major constituent of *Curcuma longa*: a review of preclinical and clinical research. Altern Med Rev. 2009; 14:141–153. [PubMed: 19594223]
17. Chiu TL, Su CC. Curcumin inhibits proliferation and migration by increasing the Bax to Bcl-2 ratio and decreasing NF-kappa Bp65 expression in breast cancer MDA-MB-231 cells. Int J Mol Med. 2009; 23:469–475. [PubMed: 19288022]
18. Liu L, Sun L, Wu Q, et al. Curcumin loaded polymeric micelles inhibit breast tumor growth and spontaneous pulmonary metastasis. Int J Pharm. 2013; 443:175–182. [PubMed: 23287774]
19. Huang MT, Lou YR, Ma W, et al. Inhibitory effects of dietary curcumin on forestomach, duodenal, and colon carcinogenesis in mice. Cancer Res. 1994; 54:5841–5847. [PubMed: 7954412]
20. Shishu, Singla AK, Kaur IP. Inhibitory effect of curcumin and its natural analogues on genotoxicity of heterocyclic amines from cooked food. Indian J Exp Biol. 2002; 40:1365–1372. [PubMed: 12974398]
21. Rinaldi AL, Morse MA, Fields HW, et al. Curcumin activates the aryl hydrocarbon receptor yet significantly inhibits (−)-benzo(a)pyrene-7R-trans- 7,8-dihydrodiol bioactivation in oral squamous cell carcinoma cells and oral mucosa. Cancer Res. 2002; 62:5451–5456. [PubMed: 12359752]
22. Song X, Siriwardhana N, Rathore K, et al. Grape seed proanthocyanidin suppression of breast cell carcinogenesis induced by chronic exposure to combined 4-(methylnitrosamino)-1-(3-pyridyl)-1-butanone and benzo[a]pyrene. Mol Carcinog. 2010; 49:450–463. [PubMed: 20146248]
23. Rathore K, Choudhary S, Odoi A, et al. Green tea catechin intervention of reactive oxygen species-mediated ERK pathway activation and chronicallyinduced breast cell carcinogenesis. Carcinogenesis. 2012; 33:174–183. [PubMed: 22045026]
24. Choudhary S, Sood S, Donnell RL, et al. Intervention of human breast cell carcinogenesis chronically induced by 2-amino-1-methyl-6- phenylimidazo[4,5-b]pyridine. Carcinogenesis. 2012; 33:876–885. [PubMed: 22307971]
25. Hanahan D, Weinberg RA. The hallmarks of cancer. Cell. 2000; 100:57–70. [PubMed: 10647931]
26. Larsson O, Zetterberg A, Engström W. Consequences of parental exposure to serum-free medium for progeny cell division. J Cell Sci. 1985; 75:259–268. [PubMed: 4044676]

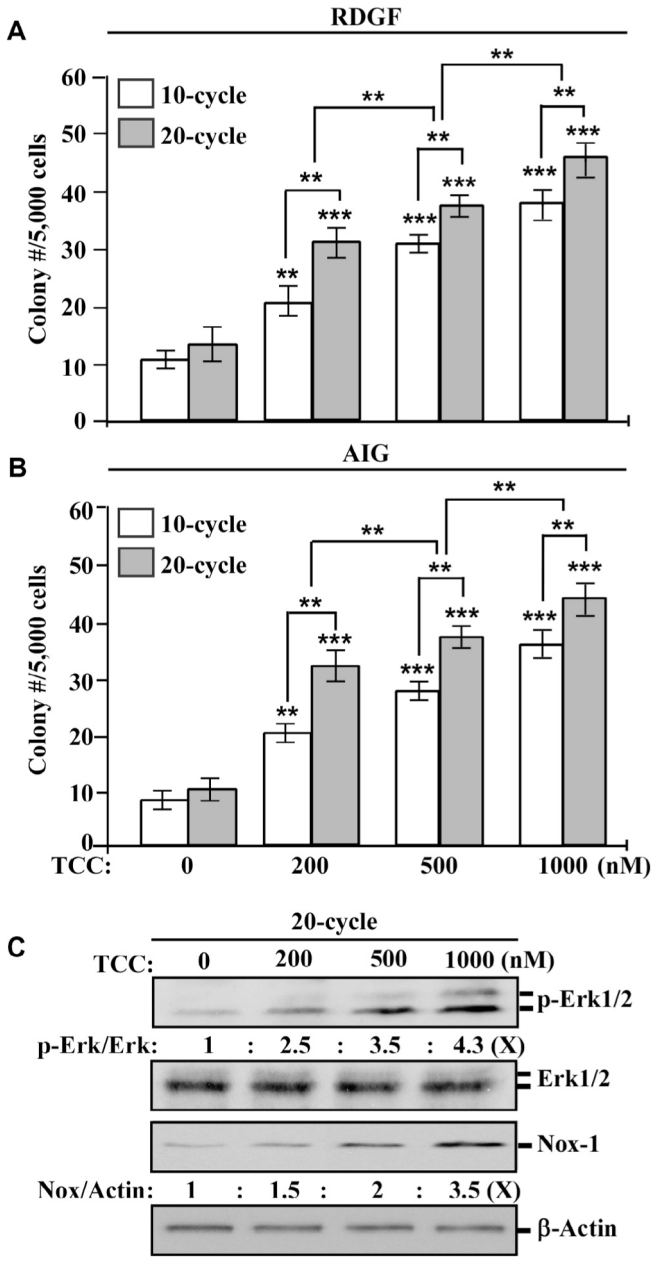

Fig. 1.

Dose- and exposure-dependent induction of carcinogenesis by TCC. MCF10A cells were repeatedly exposed to DMSO (0) or 200, 500, or 1000 nM TCC for 10 and 20 cycles. (A & B) Cellular acquisition of reduced dependence on growth factors (RDGF) and anchorage-independent growth (AIG) was determined. *Columns*, mean of triplicates; *bars*, SD. Statistical significance is indicated by $^{**}P < 0.01$, $^{***}P < 0.001$. (C) Cell lysates isolated from cultures exposed to TCC for 20 cycles were analyzed to detect levels of p-Erk1/2, Erk1/2, and Nox-1, with β-Actin as a control; these levels were quantified by densitometry. The level of specific phosphorylation of Erk1/2 (p- Erk/Erk) was calculated by normalizing the level of p-Erk1/2 with the level of Erk1/2, the level set in control cells (0 nM TCC) as 1 (X, arbitrary unit). The level of Nox-1 (Nox/Actin) was calculated by normalizing with the

level of β-Actin, the level set in control cells as 1 (X, arbitrary unit). All results are representative of three independent experiments.

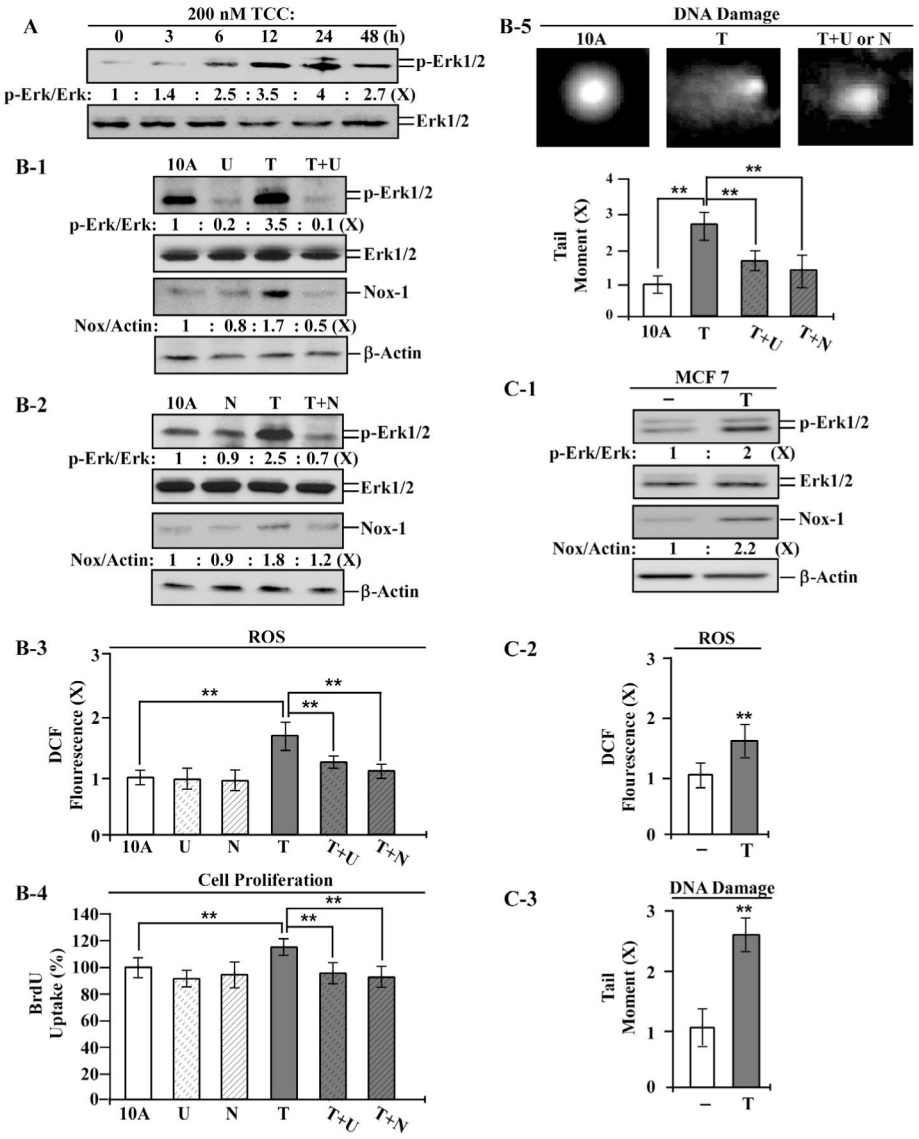

Fig. 2.

Transient endpoints induced by TCC. (A) MCF10A (10A) cells were treated with 200 nM TCC (T) for the indicated periods. (B-1 to B-5) 10A cells were exposed to TCC in the absence or presence of 10 μM U0126 (U) or 5 mM NAC (N) for 24 h. (C-1 to C-3) MCF7 cells were treated with 200 nM TCC for 24 h. (A, B-1, B-2, & C-1) Cell lysates were analyzed to detect levels of p-Erk1/2, Erk1/2, and Nox-1, with β-Actin as a control, and these levels were quantified by densitometry. The level of specific phosphorylation of Erk1/2 (p-Erk/Erk) was calculated by normalizing the level of p-Erk1/2 with the level of Erk1/2, then the level set in control cells as 1 (X, arbitrary unit). The level of Nox-1 (Nox/Actin) was calculated by normalizing with the level of β-Actin and the level set in control cells as 1 (X, arbitrary unit). (B-3 & C-2) Relative ROS levels were measured and normalized by the DCF fluorescence intensity determined in control cells, set as 1 (X, arbitrary unit). (B-4) Relative cell proliferation was determined and normalized by the value of BrdU detected in control cells, set as 100%. (B-5 & C-3) Relative DNA damage was measured by a comet assay and normalized by the value of average tail moment determined in control cells, set as 1 (X, arbitrary unit). Representative images of DNA damage in the

comet assay are shown in B5. *Columns*, mean of triplicates; *bars*, SD. Statistical significance is indicated by $^{*}P < 0.05$, $^{**}P < 0.01$. All results are representative of three independent experiments.

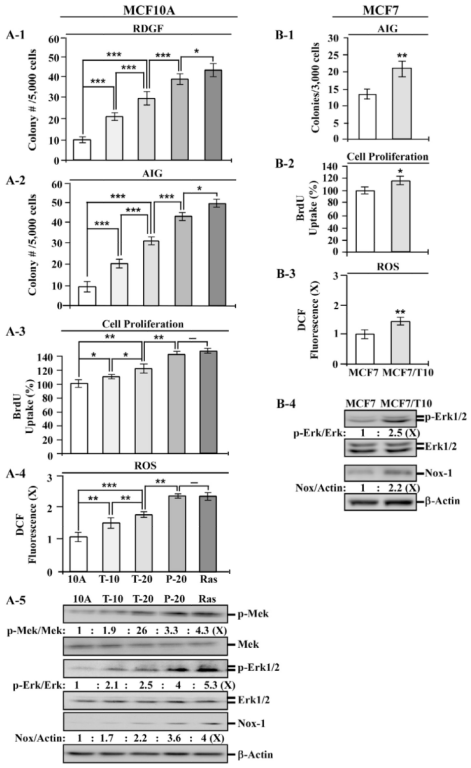

Fig. 3.

Constitutive endpoints induced by long-term exposure to TCC. MCF10A (10A) cells were repeatedly exposed to 200 nM TCC for 10 and 20 cycles, resulting in T-10 and T-20 cell lines, respectively. 10A cells were repeated exposed to 10 nM PhIP for 20 cycles to generate P-20 cells. 10A cells were stably transfected to ectopically express oncogenic H-Ras, resulting in the MCF10A-Ras cell line (Ras). MCF7 cells were repeatedly exposed to 200 nM TCC for 10 cycles, resulting in MCF7/T10 cell line. (A-1) Cellular acquisition of reduced dependence on growth factors (RDGF) was determined. (A-2 & B-1) Cellular acquisition of anchorage-independent growth (AIG) was determined. (A-3 & B-2) Relative cell proliferation was determined and normalized by the value of BrdU detected in control parental cells, set as 100%. (A-4 & B-3) Relative ROS levels were measured and normalized by the fluorescence intensity determined in control parental cells, set as 1 (X, arbitrary unit). (A-5 & B-4) Cell lysates were analyzed to detect levels of p-Mek, Mek, p-Erk1/2, Erk1/2, and Nox-1, with β-Actin as a control, and these levels were quantified by densitometry. The levels of specific phosphorylation of Mek (p-Mek/Mek) and Erk1/2 (p-Erk/Erk) were calculated by normalizing the level of p-Mek and p-Erk1/2 with the level of Mek and Erk1/2, respectively, then the level set in control parental cells as 1 (X, arbitrary unit). The level of Nox-1 (Nox/Actin) was calculated by normalizing with the level of β-Actin and the level set in control parental cells as 1 (X, arbitrary unit). *Columns*, mean of triplicates; *bars*, SD. Statistical significance is indicated by $^{*}P < 0.05$, $^{**}P < 0.01$, $^{***}P < 0.001$. All results are representative of three independent experiments.

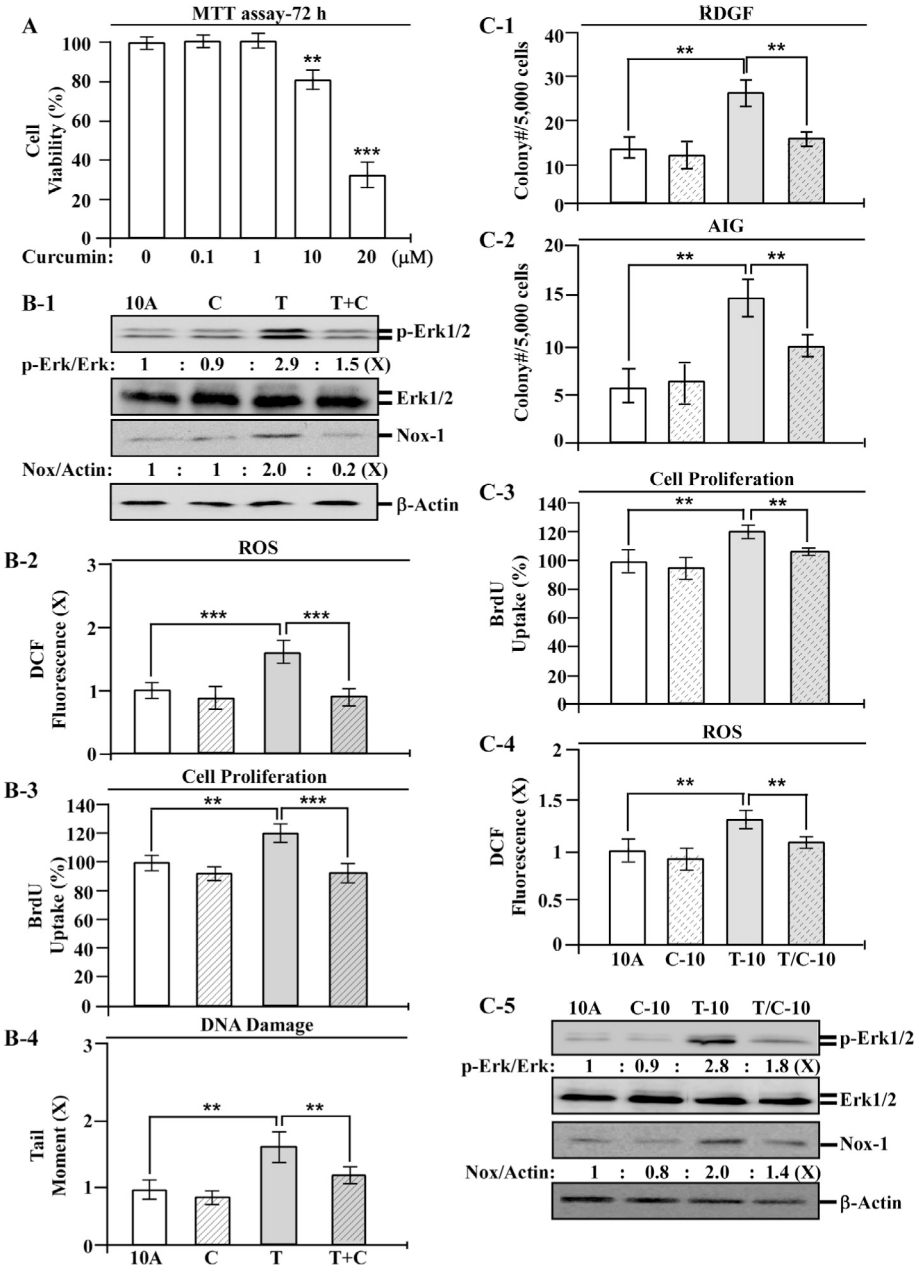

Fig. 4.

Intervention of TCC-induced carcinogenesis by curcumin. (A) MCF10A (10A) cells were treated with 0, 0.1, 10, and 20 μM curcumin for 72 h. Relative cell viability was normalized by the value determined in control cells (0 μM), set as 100%. (B-1 to B-4) MCF10A cells were treated with 200 nM TCC (T) in the absence or presence of 1 μM curcumin (C) for 24 h. (C-1 to C-4) MCF10A cells were repeatedly exposed to 200 nM TCC in the absence and presence of 1 μM curcumin for 10 cycles, resulting in 10A, C-10, T-10, and T/C-10 cell lines. (B-1 & C-5) Cell lysates were analyzed to detect levels of p-Erk1/2, Erk1/2, and Nox-1, with β-Actin as a control, and these levels were quantified by densitometry. The level of specific phosphorylation of Erk1/2 (p-Erk/Erk) was calculated by normalizing the level of p-Erk1/2 with the level of Erk1/2, then the level set in control cells as 1 (X, arbitrary

unit). The level of Nox-1 was calculated by normalizing with the level of β-Actin and the level set in control cells as 1 (X, arbitrary unit). (B-2 & C-4) Relative ROS levels were measured and normalized by the fluorescence intensity determined in control cells, set as 1 (X, arbitrary unit). (B-3 & C-3) Relative cell proliferation was determined and normalized by the value of BrdU detected in control cells, set as 100%. (B4) Relative DNA damage was measured by a comet assay and normalized by the value of average tail moment determined in control cells, set as 1 (X, arbitrary unit). (C-1) Cellular acquisition of reduced dependence on growth factors (RDGF) was determined. (C-2) Cellular acquisition of anchorage-independent growth (AIG) was determined. *Columns*, mean of triplicates; *bars*, SD. Statistical significance is indicated by $^{**}P < 0.01$, $^{***}P < 0.001$. All results are representative of three independent experiments.